Peptidomimetic Probes and Molecular Modeling Suggest That Alzheimer's γ-Secretase Is an Intramembrane-Cleaving Aspartyl Protease†

Michael S. Wolfe,*,‡ Weiming Xia,§ Chad L. Moore,‡ Dartha D. Leatherwood,‡ Beth Ostaszewski,§ Talat Rahmati,§ Isaac O. Donkor,‡ and Dennis J. Selkoe§

Department of Pharmaceutical Sciences, University of Tennessee, Memphis, Tennessee 38163, and Center for Neurologic Diseases, Harvard Medical School and Brigham and Women's Hospital, Boston, Massachusetts 02115

Received October 27, 1998; Revised Manuscript Received January 4, 1999

ABSTRACT: The amyloid β-protein (Aβ), implicated in the pathogenesis of Alzheimer's disease (AD), is a proteolytic metabolite generated by the sequential action of β- and γ-secretases on the amyloid precursor protein (APP). The two main forms of Aβ are 40- and 42-amino acid C-terminal variants, $Aβ_{40}$ and $Aβ_{42}$. We recently described a difluoro ketone peptidomimetic (**1**) that blocks Aβ production at the γ-secretase level [Wolfe, M. S., et al. (1998) *J. Med. Chem. 41,* 6−9]. Although designed to inhibit $Aβ_{42}$ production, **1** also effectively blocked $Aβ_{40}$ formation. Various amino acid changes in **1** still resulted in inhibition of $Aβ_{40}$ and $Aβ_{42}$ production, suggesting relatively loose sequence specificity by γ-secretase. The alcohol counterparts of selected difluoro ketones also lowered Aβ levels, indicating that the ketone carbonyl is not essential for activity and suggesting that these compounds inhibit an aspartyl protease. Selected compounds inhibited the aspartyl protease cathepsin D but not the cysteine protease calpain, corroborating previous suggestions that γ-secretase is an aspartyl protease with some properties similar to those of cathepsin D. Also, since the γ-secretase cleavage sites on APP are within the transmembrane region, we consider the hypothesis that this region binds to γ-secretase as an α-helix and discuss the implications of this model for the mechanism of certain forms of hereditary AD.

Accumulating biochemical, histological, and genetic evidence supports the hypothesis that the 4 kDa β-amyloid protein (Aβ)[1] is an essential component in the pathogenesis of Alzheimer's disease (AD) (*3*, *4*). Despite the intense interest in the role of Aβ in the etiology of AD, the molecular mechanism of Aβ biosynthesis is poorly understood. The 39−43-residue Aβ is formed via the sequential cleavage of the integral membrane amyloid precursor protein (APP) by β- and γ-secretases (*5*). β-Secretase cleavage of APP occurs near the membrane, producing the soluble APP_s-β and a 12 kDa C-terminal membrane-associated fragment (CTF). The latter is processed by γ-secretase, which cleaves within the transmembrane domain of the substrate to generate Aβ. An alternative proteolytic event carried out by α-secretase occurs within the Aβ portion of APP, releasing APP_s-α, and subsequent processing of the resulting membrane-bound 10 kDa CTF by γ-secretase leads to the formation of a 3 kDa N-terminally truncated version of Aβ called p3.

Heterogeneous proteolysis of the 12 kDa CTF by γ-secretase generates primarily two C-terminal variants of Aβ, 40- and 42-amino acid versions ($Aβ_{40}$ and $Aβ_{42}$), and parallel processing of the 10 kDa CTF generates the corresponding C-terminal variants of p3. Although $Aβ_{42}$ represents only about 10% of secreted Aβ, this longer and more hydrophobic variant is disproportionally present in the amyloid plaques observed post mortem in AD patients (*6*, *7*), consistent with in vitro studies illustrating the kinetic insolubility of $Aβ_{42}$ vis-à-vis $Aβ_{40}$ (*8*). Importantly, all genetic mutations associated with early-onset (<60 years) familial Alzheimer's disease (FAD) result in increased $Aβ_{42}$ production (*3*, *4*). An understanding of the production of Aβ in general and that of $Aβ_{42}$ in particular is essential for elucidating the molecular mechanism of AD pathogenesis and may also lead to the development of new chemotherapeutic agents which strike at the etiological heart of the disease.

While γ-secretase is an attractive target for inhibitor design, little is known about the structure, mechanism, or binding requirements of this unidentified protease. We recently reported that difluoro ketone peptidomimetic **1** (Figure 1) is an inhibitor of Aβ biosynthesis (*9*). The compound also caused dramatic increases in the levels of both the 10 and 12 kDa CTFs, γ-secretase substrates, but did not affect the production of α- and β-secretase-generated APP_s products. Thus, **1** inhibited Aβ biosynthesis at the level of γ-secretase. Although designed considering the cleavage site leading to $Aβ_{42}$ (Figure 1), **1** more potently inhibited $Aβ_{40}$ production in human embryonic kidney (HEK) 293 cells. More recently, **1** was found to inhibit Aβ production in a cell-free system (*10*), consistent with direct binding to γ-secretase. From this prototype substrate-based inhibitor, related analogues were designed to test hypotheses concerning the nature of the substrate/γ-secretase interaction and

† This work supported by NIH Grants NS 37537 (M.S.W.), HL 3536 (I.O.D.), and AG 12749 (D.J.S.) and a Faculty Development Grant from the University of Tennessee College of Pharmacy (M.S.W.).

* To whom correspondence should be addressed. Telephone: (901) 448-7533. Fax: (901) 448-6828. E-mail: mwolfe@utmem.edu.

‡ University of Tennessee.

§ Harvard Medical School and Brigham and Women's Hospital.

[1] Abbreviations: Aβ, β-amyloid protein; $Aβ_{40}$, 40-amino acid variant of β-amyloid protein; $Aβ_{42}$, 42-amino acid variant of β-amyloid protein; AD, Alzheimer's disease; APP, amyloid precursor protein; CHO, Chinese hamster ovary; CTF, C-terminal fragment; FAD, familial Alzheimer's disease; HEK, human embryonic kidney; SREBP, sterol regulatory element-binding protein; S2P, sterol regulatory element-binding protein site 2 protease.

10.1021/bi982562p CCC: $18.00
Published on Web 03/26/1999

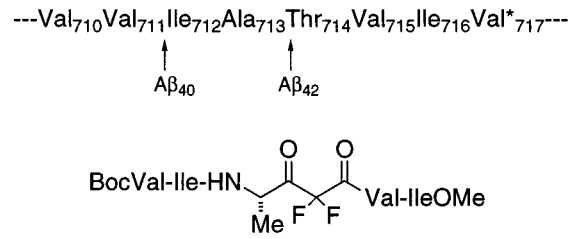

FIGURE 1: Amino acid sequence in and around the γ-secretase cleavage sites leading to Aβ_{40} and Aβ_{42} and the structure of substrate-based γ-secretase inhibitor **1**. The asterisk denotes a site of mutation associated with FAD.

to identify the protease class to which γ-secretase belongs.

In this report, we describe the effects of structural modifications of **1** on the inhibition of Aβ_{40} and Aβ_{42} formation. The structure−activity relationships are consistent with loose sequence specificity at the active site of γ-secretase. Selected compounds did not inhibit the cysteine protease calpain but did inhibit the aspartyl protease cathepsin D. In addition, NMR studies indicate that the difluoro ketones are almost entirely in the hydrate form in the presence of small amounts of D_2O, and the alcohol counterparts of selected ketones retained inhibitory effects on Aβ production. Taken together, these results suggest that the difluoro ketones are active as hydrates and that γ-secretase is an aspartyl protease with some cathepsin D-like properties. We also consider, through molecular modeling and inhibitor design, the hypothesis that the apparently intramembranous cleavage site of APP binds to γ-secretase in an α-helical conformation and discuss the implications of this model for the molecular mechanism of FAD.

EXPERIMENTAL PROCEDURES

General Synthetic Methodology for Peptide Analogues. The various difluoro ketone peptidomimetics were synthesized through modification of procedures described previously (*9*). *N*-Boc-protected L-alanine and valine aldehydes were obtained with high enantiomeric purities (>99%) from the corresponding *N*-Boc-protected L-amino acid via their Weinreb amides (*11*). The aldehyde was added to activated zinc and ethyl bromodifluoroacetate in THF under reflux conditions for 30 min to provide the key difluoro alcohol intermediate. This intermediate was hydrolyzed with 1 equiv of 0.25 N NaOH in an equal volume of acetonitrile for 1.5 h, and the free C-terminus was coupled to a di- or tripeptide *O*-methyl ester overnight using 1.1 equiv of *N*-[(dimethylamino)-1*H*-1,2,3-triazolo[4,5-*b*]pyridin-1-ylmethylene]-*N*-methylmethanaminium hexafluorophosphate *N*-oxide (HATU, Perseptive Biosystems) in the presence of 3 equiv of diisopropylethylamine (DIEA) in DMF. After removal of the Boc protecting group with 50% TFA in CH_2Cl_2, the N-terminus was sequentially coupled with *N*-Boc amino acids via HATU and DIEA to obtain the penultimate difluoro alcohols. Oxidation with 3.5 equiv of Dess−Martin periodinane reagent in CH_2Cl_2 for 3 h yielded the difluoro ketone final products. All final compounds and their intermediates were characterized and assessed for purity by melting point, ^{1}H NMR (300 MHz), mass spectrometry (MALTI-TOF), and elemental analysis (Desert Analytics, Tucson, AZ).

Cell Lines, Compound Treatments, and ELISAs. Cell lines were Chinese hamster ovary (CHO) and SK-N-SH human neuroblastoma cells stably transfected with the 751- or 695-amino acid splicing variants of APP, respectively, and the *neo* gene, and human embryonic kidney (HEK) 293 cells carrying the same genes (APP695 plus *neo*) but with the K595N/M596L ("Swedish") double mutation of APP (*12*, *13*). Cells were grown to confluence in Dulbecco's modified Eagle's medium containing 200 μg/mL G418 (Gibco BRL). Stock concentrations of the peptide analogues in DMSO were added to media to reach the final concentrations with 1% DMSO. Positive controls contained 1% DMSO alone. After 4 h, the medium was removed and centrifuged at 3000*g* for 5 min, and the supernatant was stored at −80 °C until the assays were carried out. Sandwich ELISAs for Aβ_{40} and Aβ_{42} were performed as described previously (*14*, *15*). The capture antibodies were 2G3 (to Aβ_{40} residues 33−40) for the Aβ_{40} species and 21F12 (to Aβ_{42} residues 33−42) for the Aβ_{42} species. The reporter antibody was biotinylated 3D6 (to Aβ residues 1−5) in each assay. Horseradish peroxidase−avidin binding to the reporter antibody was detected using 3,3′,5,5′-tetramethylbenzidine (Pierce), measuring at 455 nm for calculating Aβ levels and at 595 nm for normalization.

Assays for Calpain and Cathepsin D Inhibition. Inhibition of rabbit skeletal muscle calpain (Sigma) was assessed using a previously described assay procedure (*16*). Briefly, a mixture containing 2 μg/mL casein, 50 mM Tris-HCl (pH 7.4), 10 mM DTT, 4.2 μg of *m*-calpain, and 10 mM $CaCl_2$ was incubated in a total volume of 500 μL for 30 min at 25 °C. Duplicate 25 μL aliquots of the assay mixture were each diluted with 800 μL of water, treated with 200 μL of Bio-Rad dye reagent concentrate, and vortexed. After 10 min, the absorbance at 595 nm was determined, and calpain activity was expressed as the difference in absorbance at 595 nm between identical samples with or without $CaCl_2$. Calpain inhibitor I (Calbiochem) was used as a standard inhibitor.

The assay of bovine spleen cathepsin D (Sigma) was performed according to the manufacturer's protocol with modification. A reaction cocktail containing 2.5% hemoglobin solution, 400 mM citrate buffer, and water (4:1:4) was equilibrated at 37 °C and adjusted to pH 3.0. The reaction cocktail (970 μL) was mixed with 20 μL of DMSO containing inhibitor at varying concentrations and 0.022 unit of cathepsin D in 10 μL of water. After incubation at 37 °C for 30 min, the reaction was quenched with 1 mL of 5% TCA and the mixture passed through a 0.45 μm syringe filter and measured for absorbance at 280 nm. For blanks, TCA was added before the enzyme. Pepstatin (Sigma) was used as a standard inhibitor.

Molecular Modeling. All molecular modeling studies were conducted using the program SYBYL 5.5 (Tripos Associates) running on a Silicon Graphics Iris workstation. The postulated APP transmembrane region (amino acids 700−723 in the 770-amino acid splice variant numbering, GAIIGLMVGGVVIATVIVITLVML) was constructed with idealized ϕ and φ values of −58° and −47°, respectively. Energy minimization using the Kollman all-atom force field left the conformation essentially unaffected. The conformations of SYBYL-constructed peptide analogues were manually altered to attain apparent overlap with the APP transmembrane helix and then energy minimized. Compound **1** was further analyzed; 10 energy minima were obtained through a computational "annealing" process, iteratively heating to 500 K and cooling to 200 K. The 10 conformers so generated were then each minimized.

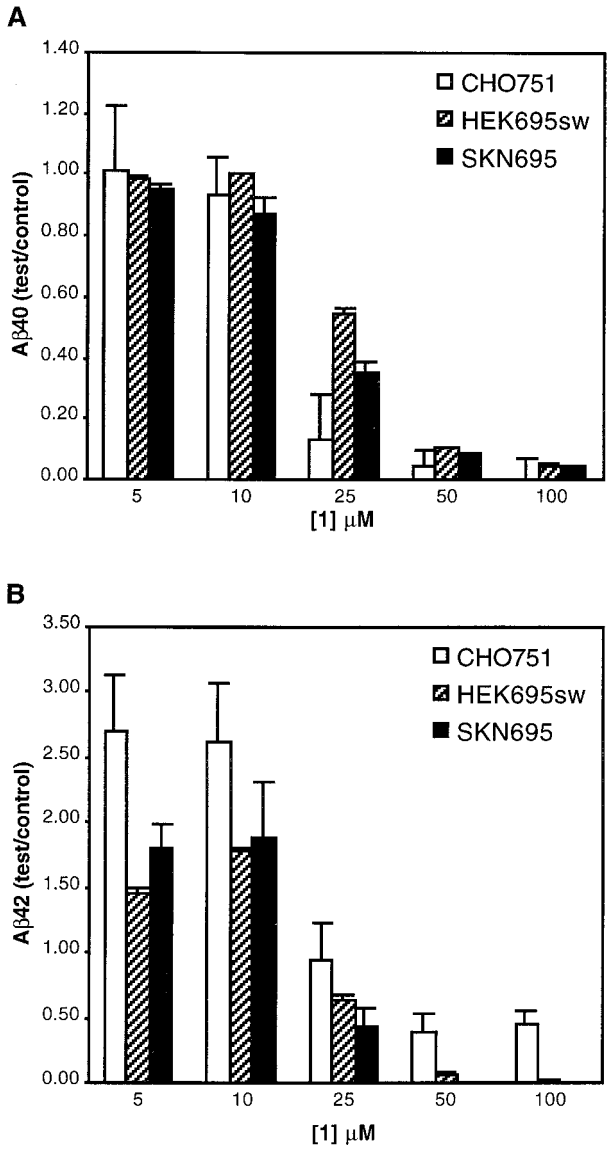

FIGURE 2: Effects of difluoro ketone peptidomimetic **1** on Aβ production as determined by sandwich ELISA. (A) Effects of **1** on Aβ_{40} production after 4 h of treatment of CHO and SK-N-SH cells stably transfected with the 751- and 695-amino acid splice variants of APP (CHO751 and SKN695) and of HEK 293 cells stably transfected with the K595N/M596L (Swedish) double mutation of APP695 (HEK695sw). (B) Effect of **1** on Aβ_{42} production in these same cell lines. Aβ levels are expressed as a ratio of Aβ present in medium after 4 h in the presence of **1** in 1% DMSO vs that in 1% DMSO alone ($n = 2$).

RESULTS

*Effects of Inhibitor **1** on Aβ_{40} and Aβ_{42} Production As Assessed by the Sandwich ELISA.* In our previous report of the inhibitory properties of **1** on γ-secretase activity (*9*), we initially assessed the effects of the compound on Aβ production by [^{35}S]methionine labeling, immunoprecipitation with C-terminally specific antibodies, and analysis by SDS−PAGE. This procedure is inconvenient for screening numerous compounds, and so we now routinely employ a rapid, sensitive, and quantitative double antibody enzyme-linked immunosorbent assay (sandwich ELISA) (*14*, *15*) in human APP-transfected Chinese hamster ovary (CHO) cells to determine the extent of inhibition of Aβ formation (Figure 2). As we observed in HEK cells by immunoprecipitation/SDS−PAGE (*9*), **1** inhibited Aβ_{40} production more effectively than that of Aβ_{42}; at 25 μM of **1**, Aβ_{40} formation was considerably blocked, while the level of Aβ_{42} was indistinguishable from that of the control. However, at lower concentrations, **1** induced a 2−3-fold rise in the level of Aβ_{42} production [also previously seen by immunoprecipitation/SDS−PAGE (*9*)]. This effect on Aβ_{42} at lower concentrations has also been observed with peptide aldehyde γ-secretase inhibitors (*13*, *17*). Similar effects of **1** were seen by the ELISA in HEK 293 cells transfected with the K595N/M596L (Swedish) double mutation of APP and in SK-N-SH human neuroblastoma cells transfected with APP (Figure 2); Aβ_{40} production was inhibited, albeit somewhat less effectively, and Aβ_{42} levels were substantially increased at 5−10 μM **1**. However, Aβ_{40} and Aβ_{42} production were both inhibited about 50% at 25 μM in the HEK and SK-N-SH. Using radiolabeling, immunoprecipitation, and SDS−PAGE, we had previously observed inhibition of Aβ_{42} production in HEK cells by **1** only over 100 μM (*9*). The reason for the apparent discrepancy in Aβ_{42} inhibition in HEK cells between the immunoprecipitation/SDS−PAGE and ELISA methods is not clear, but may be because, in the former method, cells were pulsed with [^{35}S]methionine for 2 h and then chased for 2 h in the presence of **1**. The half-life of APP in cells is ~30 min (*18*), and Aβ_{42} is primarily formed in the endoplasmic reticulum (*19*−*21*). Thus, accumulated intracellular Aβ_{42} generated during the pulse period cannot be inhibited by **1**, and the sandwich ELISA results may better reflect inhibitory potency toward this Aβ variant. Controls showed that **1** did not interfere with the ability of antibodies to detect either Aβ_{40} or Aβ_{42} in conditioned media. With respect to cytotoxicity, up to 100 μM **1** did not affect secretion of either APP$_s$-α or -β (*9*) and did not result in any apparent change in cell morphology. Thus, the highest concentrations of **1** examined did not reduce Aβ production through a general metabolic disturbance.

Effects of Other Difluoro Ketone Peptidomimetics Designed as Inhibitors of Aβ_{42} Production Considering the Linear Sequence around the Cleavage Site. In an attempt to reverse the selectivity or improve the potency for inhibiting Aβ_{42} production, we made several changes in the structure of **1** on the basis of the linear sequence of APP immediately flanking the site of cleavage leading to this C-terminal isoform. These residues are highly hydrophobic, since this region of APP lies within the transmembrane domain. Position 717 (numbering of the 770-amino acid splicing variant of APP) is in the P4′ site. Three different mutations in this position (V717F, V717I, and V717G) cosegregate with FAD in certain families, and all three lead to specific increases in Aβ_{42} production (*22*). If the increased Aβ_{42} production is due to better binding to a separate "γ(42)-secretase" by these mutated substrates, then peptide analogues with these mutant residues installed in the appropriate position might inhibit such a γ-secretase isoenzyme more potently. Thus, we synthesized **2**, a C-terminally extended version of **1** with a residue representing the wild-type P4′ residue, Val717 (Chart 1). Being longer and more hydrophobic, **2** was poorly soluble and inappropriate for further study. However, we found that the N-terminal valine of **1** was not essential for activity; the truncated analogue **3** possessed inhibitory properties similar, if not superior, to those of **1** (Figure 3). Therefore, the C-terminally extended

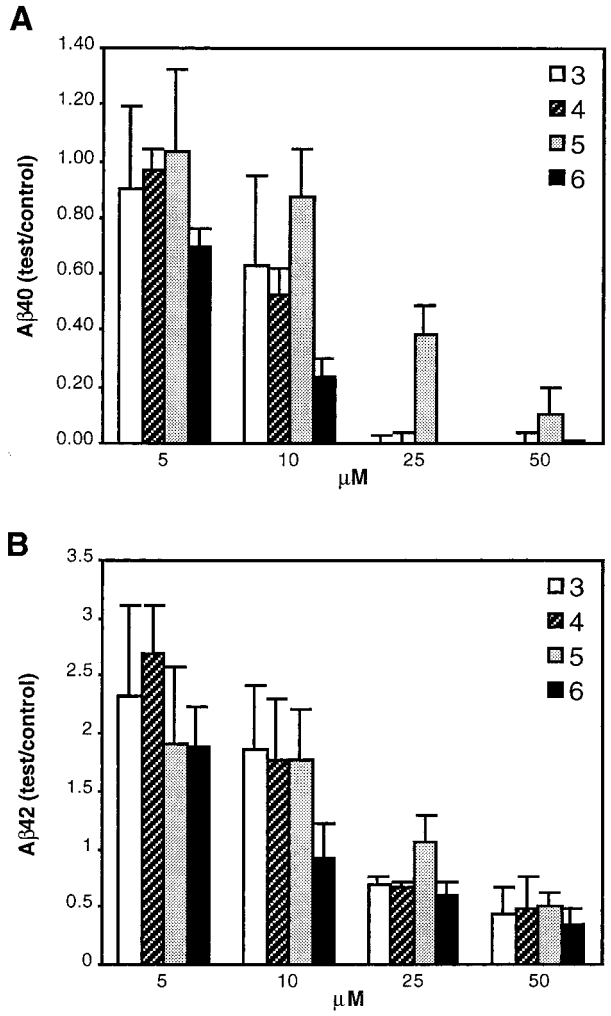

FIGURE 3: Effect of difluoro ketone peptidomimetics **3**−**6** (A) on $A\beta_{40}$ production and (B) on $A\beta_{42}$ production after 4 h in the CHO751 cells as determined by a sandwich ELISA ($n = 4$).

Chart 1

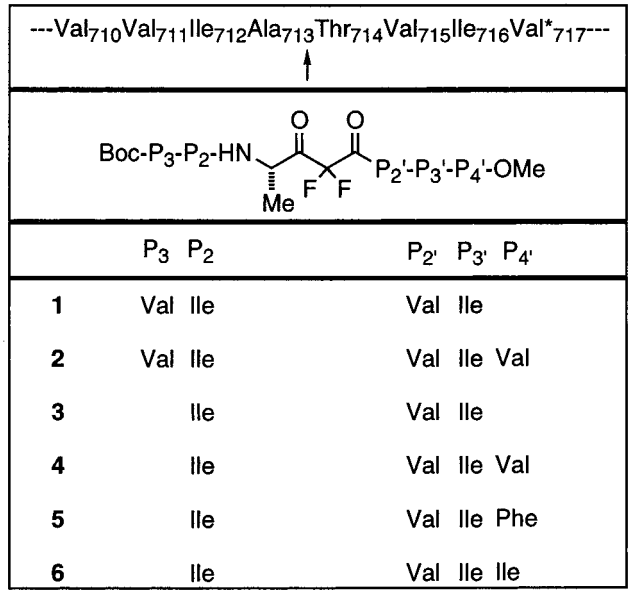

	P_3	P_2	$P_{2'}$	$P_{3'}$	$P_{4'}$
1	Val	Ile	Val	Ile	
2	Val	Ile	Val	Ile	Val
3		Ile	Val	Ile	
4		Ile	Val	Ile	Val
5		Ile	Val	Ile	Phe
6		Ile	Val	Ile	Ile

version of **3** was synthesized, and this compound (**4**) was sufficiently soluble for study in the cell-based assay. The activity of **4** was essentially the same as that of its shorter counterpart **3**. Installation of phenylalanine in the P4′ site (**5**) led to reduced activity, while isoleucine in this position (**6**) improved activity. However, neither replacement of the C-terminal valine reversed selectivity in favor of inhibiting $A\beta_{42}$ formation. In fact, as previously observed with **1**, each of these compounds induced increases in $A\beta_{42}$ production at lower concentrations. These increases are apparently not due to cytotoxic effects; as noted above for **1**, no changes in cell morphology were seen upon treatment with these compounds or with those discussed below.

Observations upon Considering an α-Helical Model of the APP Transmembrane Region. The above findings led us to consider other hypotheses concerning the nature of the interaction between γ-secretase and its substrates. The cleavage sites for γ-secretase lie in the middle of the postulated transmembrane domain of APP (*22*). Does this proteolysis actually take place within the membrane? Although recent reports describe three other proteins thought to be cleaved within their transmembrane domains (*23*−*25*), it is not known whether the substrates are somehow dislodged from the membrane, exposing them to proteases, or whether they are processed via an unprecedented intramembranous proteolysis. Since transmembrane regions of proteins typically assume an α-helical conformation, we constructed the APP transmembrane domain in this conformation using the molecular modeling software program SYBYL to determine if this could provide insight into the nature of the APP/γ-secretase interaction.

Two major observations were gleaned from this model. First, the γ-secretase cleavage sites leading to $A\beta_{40}$ and $A\beta_{42}$ are located on opposite sides of the helix (Figure 4A); when looking at the $Ala_{7.3}$−Thr_{714} amide bond hydrolyzed to generate $A\beta_{42}$ (Figure 4A, left), the helix must be rotated almost 180° to observe in the same way the Val_{711}−Ile_{712} amide bond hydrolyzed to generate $A\beta_{40}$ (Figure 4A, right). Second, the side chain of residue 717 is immediately adjacent to the Ala_{713}−Thr_{714} amide bond. In this model, it is easy to appreciate how mutation at position 717, as observed in certain FAD cases, could influence cleavage at the Ala_{713}−Thr_{714} bond to alter $A\beta_{42}$ production. In an extended model of this region of APP, position 717 is not so close to the site of cleavage leading to $A\beta_{42}$ formation, and it is difficult to understand why mutation in this particular position, representing P4′, would lead to specific increases in $A\beta_{42}$.

The α-helical model of the transmembrane region seemed to explain why compound **1**, designed considering the cleavage site leading to $A\beta_{42}$, was effective at inhibiting $A\beta_{40}$ formation. When **1** was manually overlaid onto the face of the helix with the cleavage site leading to $A\beta_{40}$ and energy minimized, considerable overlap could be achieved (Figure 4B). Considering the calculated energy of this conformer (14.98 kcal/mol) and the energy of the global minimum (10.36 kcal/mol), the depicted conformer should be energetically attainable. Moreover, one local energy minimum of **1** had a conformation similar to that of the conformer depicted in Figure 4B, again suggesting that the depicted conformation can be attained by **1**. Note the overlap of the compound with Val_{707}, Val_{715}, and Ile_{718} and the proximity of the difluoroketone moiety with the scissile Val_{711}−Ile_{712} amide bond. Although the P1 methyl substituent of **1** appears to be suboptimal for mimicking the isopropyl group of Val_{711}, we thought the flanking residues might confer the ability of this compound to inhibit $A\beta_{40}$ production.

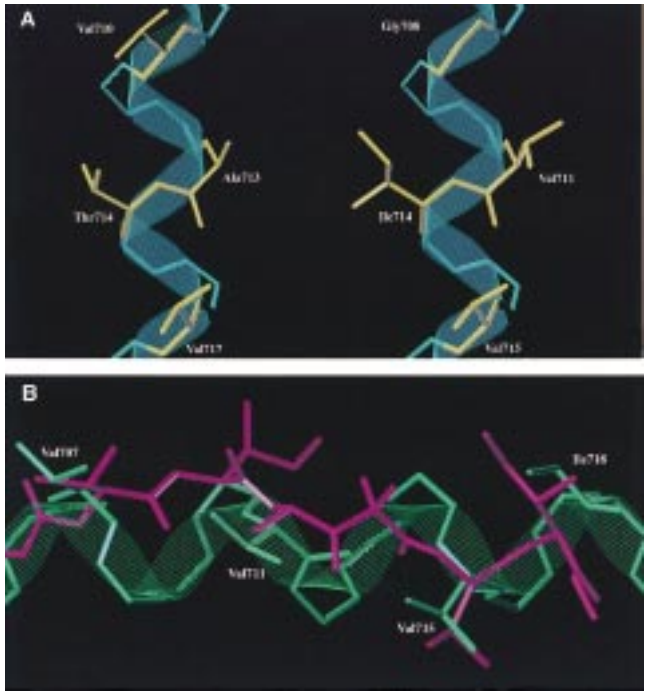

FIGURE 4: (A) α-Helical model of the APP transmembrane region. The left side depicts the face of the helix containing the Ala_{713}−Thr_{714} scissile amide bond. Note the proximity of the Val_{717} position, mutated in certain forms of FAD, to this cleavage site leading to Aβ_{42}. The right side depicts the same model rotated 180°, illustrating the Val_{711}−Ile_{712} scissile amide bond, the site of cleavage leading to Aβ_{40}. Residues on the α-helical face of interest are yellow. (B) Overlay of compound **1** (magenta) onto the face of the helix containing the cleavage site of APP leading to Aβ_{40} (blue-green). Only the APP helical backbone is shown, except for residues that **1** was postulated to mimic.

To test this idea, related difluoroketone peptidomimetics **7**−**12** (Chart 2) were designed considering this α-helical model. Because Val_{710} is positioned close to the scissile Ala_{713}−Thr_{714} bond (see Figure 4A, left), this residue was installed on the N-terminal portion (position P2) of the pseudodipeptide difluoro ketone moiety (compounds **7**, **9**, and **11**). Molecular modeling illustrated that an analogue with D-Val installed in this N-terminal position was capable of overlapping well onto the face of the APP α-helix with the cleavage site leading to Aβ_{42} even after energy minimization, and so D-Val counterparts **8**, **10**, and **12** were synthesized as well. Because position 717 also lies immediately adjacent to the Ala_{713}−Thr_{714} amide bond in the α-helical model and V717F mutations cosegregate with FAD, the Val on the C-terminal portion of the difluoro ketone unit of **7** and **8** (position P2′) was replaced with Phe in **9** and **10**. In addition, we synthesized two analogues (**11** and **12**) with an isopropyl substituent in the difluoro ketone moiety. This substituent was designed to mimic the P1 valine residue in Aβ_{40} generation, with the idea that its installation might improve selectivity for inhibition of this Aβ variant.

We found that **7** and **11** were the most active compounds in this series, comparable to prototype inhibitor **1** and its truncated version **3** (Figure 5, 25 μM). Surprisingly, these two compounds displayed similar potencies and selectivities for inhibition of Aβ_{40} and Aβ_{42} production, indicating relatively loose sequence specificity in position P1. The installation of Phe in position P2′ either did not improve activity (**8** vs **10**) or reduced activity (**7** vs **9**). Inverting the

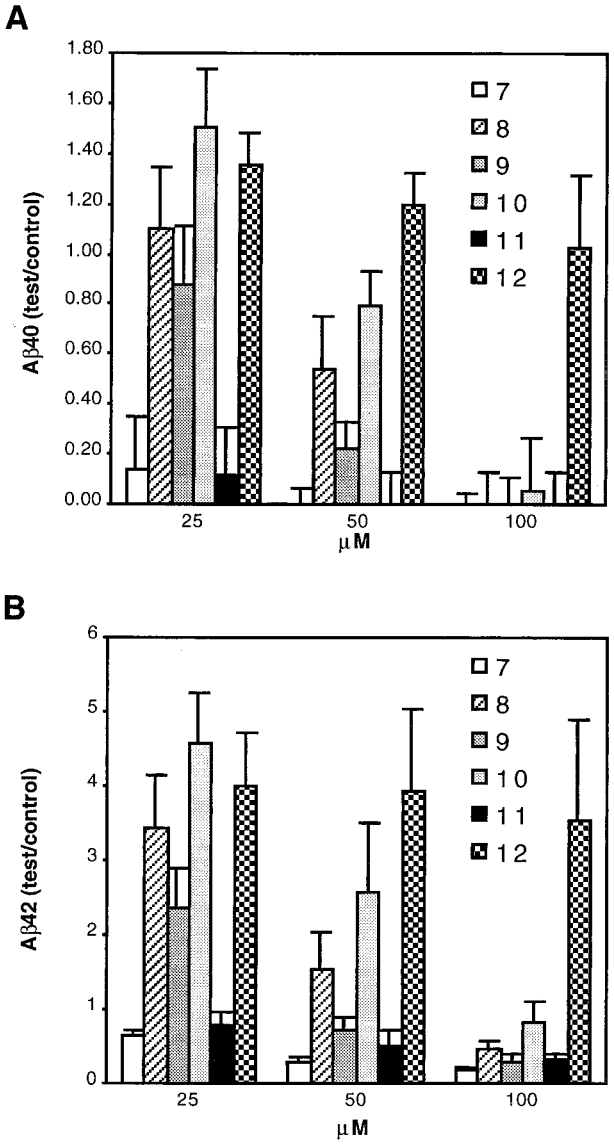

FIGURE 5: Effect of difluoro ketone peptidomimetics **7**−**12** (A) on Aβ_{40} production and (B) on Aβ_{42} production after 4 h in CHO751 cells as determined by a sandwich ELISA ($n = 4$).

Chart 2

$Val_{710}Val_{711}Ile_{712}Ala_{713}Thr_{714}Val_{715}Ile_{716}Val^{*}_{717}Ile_{716}$

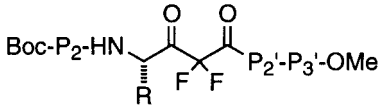

	P_2	R	$P_{2'}$	$P_{3'}$
7	Val	Me	Val	Ile
8	D-Val	Me	Val	Ile
9	Val	Me	Phe	Ile
10	D-Val	Me	Phe	Ile
11	Val	i-Pr	Val	Ile
12	D-Val	i-Pr	Val	Ile

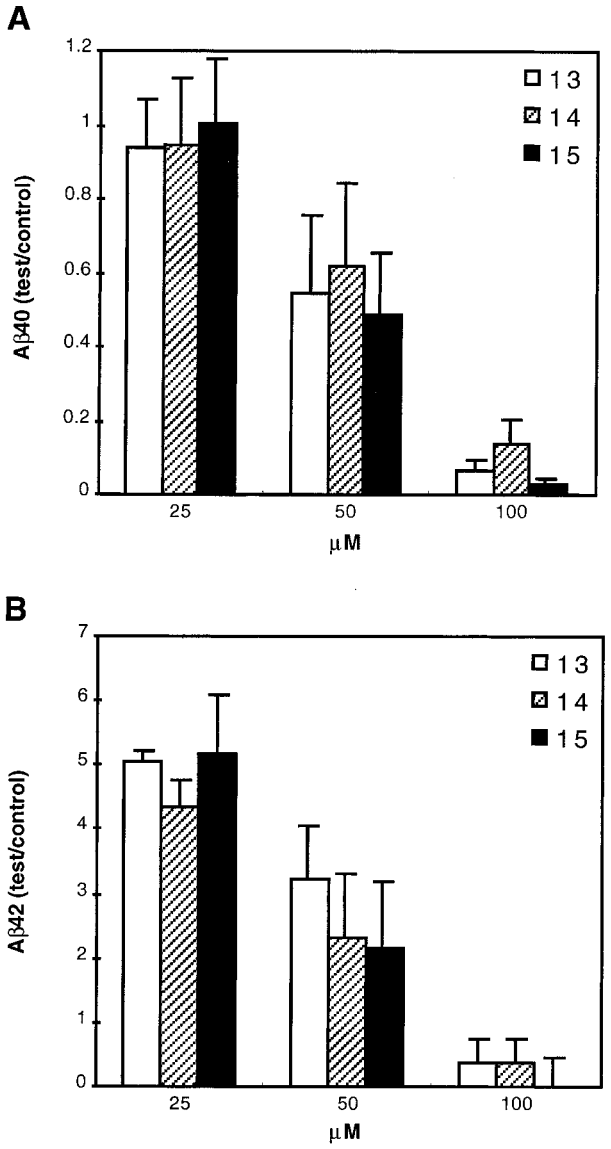

FIGURE 6: Effect of difluoro alcohol peptidomimetics **13**−**15** (A) on Aβ_{40} production and (B) on Aβ_{42} production after 4 h in CHO751 cells as determined by a sandwich ELISA ($n = 4$).

stereochemistry of the P2 Val (**7** vs **8**, **9** vs **10**, and **11** vs **12**) invariably led to less effective compounds. The rank orders of potency for inhibiting Aβ_{40} and Aβ_{42} are quite similar. Despite our designing them to mimic the cleavage site leading to Aβ_{42} formation, none of the compounds reversed selectivity in favor of inhibiting production of this Aβ variant; indeed, as with the compounds in Chart 1, **7**−**12** all induced increased levels of Aβ_{42} at lower concentrations [**7** and **11** caused 2−3-fold increases in the Aβ_{42} level at 5−10 μM (not shown)]. While altering the structure of the compounds leads to clear differences in potency, what is particularly notable is that these various changes are largely tolerated by the γ-secretases; all the tested compounds in Charts 1 and 2 except **12** inhibit Aβ production at 100 μM. The alcohol counterparts of **1**, **7**, and **11** (designated **13**−**15**, respectively; *R* stereochemistry at the carbinol) were also tested for their ability to affect Aβ production. Although less effective than the ketones, **13**−**15** were capable of inhibiting Aβ production as well (Figure 6), indicating that while the ketone functionality increases activity, it is not essential. In our previous report (*9*), inhibition of Aβ by **13** in HEK cells was not observed, but the ELISA method employed in the study presented here is more sensitive and probably more reflective of a compound's inhibitory potency than the radiolabeling/immunoprecipitation protocol used in the earlier report (vide supra).

Table 1: Inhibition of Cathepsin D Activity and Aβ Production by Selected Compounds

compound	IC_{50} vs cathepsin D (μM)	IC_{50} vs Aβ production (μM)[a]
1	0.050 ± 0.015	10−25
3	>10	10−25
4	2.3 ± 0.4	10−25
7	>10	10−25
11	2.6 ± 1.2	10−25
13	0.043 ± 0.007	50−100
15	>10	25−50

[a] Concentration ranges for IC_{50} values vs Aβ_{40} production in CHO cells stably transfected with APP695 (taken from Figures 2, 3, 5, and 6).

Previously reported peptide aldehydes that block Aβ formation at the γ-secretase level (*13*, *17*, *26*) also inhibit the calcium-activated cysteine protease calpain (*27*, *28*). When we tested selected difluoro ketone peptidomimetics (**1**, **3**, **4**, **7**, and **11**) for calpain inhibition, we found these compounds to be essentially inactive ($IC_{50} \geq 100$ μM). Thus, it is possible to inhibit γ-secretase activity without inhibiting calpain. Because it has been suggested that γ-secretase is a cathepsin D-like protease (*29*, *30*) and difluoro ketones and difluoro alcohols have been reported to inhibit cathepsin D (*31*), we also tested selected compounds for inhibition of this aspartyl protease (Table 1). Some compounds were capable of inhibiting cathepsin D, with **1** being quite potent ($IC_{50} = 50$ nM). However, it is notable that activity against cathepsin D is not predictive of activity against γ-secretase. For example, compound **3** is inactive against cathepsin D ($IC_{50} > 10$ μM), yet this peptidomimetic is essentially equipotent with respect to **1** in blocking Aβ production (Table 1).

DISCUSSION

Other than difluoro ketone **1**, only four compounds have been reported as inhibitors of γ-secretase (*13*, *17*, *26*). There is no evidence that any of these peptide aldehyde inhibitors directly interact with γ-secretase, due to the lack of a suitable in vitro assay for these as yet unidentified proteases. Recently, we have observed that **1** inhibits Aβ production in a cell-free microsomal system (*10*), consistent with the hypothesis that this compound, designed to mimic a γ-secretase cleavage site, interacts directly with γ-secretase. Thus, **1** and analogues thereof could serve as molecular probes for the active site of this enzyme.

An advantage of the difluoro ketone peptidomimetics over the peptide aldehydes is that the former allow exploration of the importance of residues on the "prime side" (C-terminal side) of the cleavage site. Hence, we could test the hypothesis that position 717 is an important determinant in the direct interaction between APP CTFs and a putative γ(42)-secretase. Once we had established that the P3 valine of **1** is not essential to activity (**3** retained activity) and could be omitted, compounds that extended into position P4′ to mimic position 717 and yet possessed manageable solubility properties were obtained (**4**−**6**). However, such extension to

position P4′ did not result in reversal of selectivity in favor of inhibiting Aβ_{42} formation.

Because the γ-secretase cleavage sites lie within the transmembrane region of APP and transmembrane regions of proteins typically assume an α-helical conformation, we considered this conformation for the APP transmembrane domain. In this model, the cleavage sites leading to Aβ_{40} and Aβ_{42} are on opposite faces of the helix, and position 717 is immediately adjacent to the amide bond cleaved in the generation of Aβ_{42} but not to the amide bond hydrolyzed during the formation of Aβ_{40}. Several mutations in this position cause FAD and specifically lead to increased production of Aβ_{42} (*3*, *4*). Thus, the α-helical model provides a simple explanation for how mutations in the APP 717 position might cause FAD through increased Aβ_{42} production; such changes would be expected to affect the binding (K_m) of this face of the helix to γ-secretase or the rate of its cleavage once bound (V_{max}).

The flanking residues of the truncated difluoro ketone analogue **3** were altered considering the α-helical model. None of the compounds reversed the selectivity to favor Aβ_{42} inhibition, although in general these compounds retained activity. It is intriguing that installation of a valine side chain (i.e., isopropyl group) into the P1 site of the difluoro ketone peptidomimetics did not lead to more selective inhibition of Aβ_{40} formation, as one might expect upon inspection of the cleavage site leading to this Aβ variant. Conclusions concerning the γ-secretase active site from these results are tentative, because differences in cell penetration and metabolism among these compounds may also be factors. Nevertheless, the results are consistent with γ-secretase having loose sequence specificity, a conclusion corroborated by recent site-directed mutagenesis studies on APP near the γ-secretase cleavage sites (*32*−*34*). The apparent loose sequence specificity runs counter to our initial hypothesis concerning the importance of the flanking residues in determining specificity (see Figure 4B and the accompanying text in the Results). Interestingly, Aβ_{40} and Aβ_{42} production are inhibited by these peptidomimetics with the same rank order of potency, suggesting that they are generated from γ-secretases with similar active site topographies.

The increased level of Aβ_{42} production observed at lower concentrations of the peptidomimetics, also reported for other γ-secretase inhibitors (*13*, *17*), remains mysterious. Although calpain inhibition can result in augmented Aβ_{42} secretion (*35*), the mechanism for this increase induced by the difluoro ketone analogues reported here must be different since they are not effective against calpain. Further studies toward understanding the nature of these Aβ_{42} increases are warranted because these pharmacologically induced increases mirror the effects of FAD-causing APP and presenilin mutations on Aβ formation (*3*, *4*). Such an understanding would also facilitate the development of clinically useful γ-secretase inhibitors that reduce Aβ_{42} more effectively.

The difficulty in selectively inhibiting γ(42)-secretase activity may be due to the principal intracellular location of Aβ_{42} production: early secretory compartments, including the endoplasmic reticulum and Golgi (*19*−*21*). The current inhibitors may concentrate more in the endosomal/lysosomal pathway and/or in the trans-Golgi network where Aβ_{40} production may occur (*21*, *36*). Selective inhibition of Aβ_{40} formation may then lead to more substrate being available for Aβ_{42} formation. However, certain inhibitors caused large increases in the level of Aβ_{42} without decreasing the level of Aβ_{40} at the same dose (Figure 5, compounds **10** and **12**). Although the reason for the increased Aβ_{42} level induced by these compounds is unclear, this observation nevertheless provides further evidence for pharmacologically distinct γ-secretase activities (*13*).

Unlike the reported peptide aldehyde γ-secretase inhibitors, the difluoro ketone peptidomimetics examined here were not effective against calpain. They did, however, inhibit the aspartyl protease cathepsin D. Although cathepsin D has been suggested as a γ-secretase candidate (*29*, *30*), deleting the cathepsin D gene does not result in lower Aβ levels (*37*). Thus, it is clear that cathepsin D per se is not γ-secretase, but these two proteases apparently possess some similar properties. Inhibition of aspartyl proteases by difluoro ketones is known to occur through the hydrated form of the ketone (*38*−*41*), which closely mimics the gem-diol intermediate in the catalytic mechanism. In contrast, inhibition of serine proteases by difluoro ketones (*42*) and of cysteine proteases by fluoromethyl ketones (*43*) proceeds via nucleophilic attack by the active site serine or cysteine to produce a stable, covalently linked hemiacetal or hemithioacetal enzyme−inhibitor complex. Such complexes cannot be formed with difluoro alcohols. ^{1}H NMR data reveal that the difluoroketone inhibitors reported here are readily converted to the hydrate form in the presence of small amounts of D_2O (ref *9* and data not shown). Furthermore, while the difluoro ketone inhibitors are more potent than the corresponding alcohols, the fact that the alcohols still possess activity indicates that the ketone functionality is not essential and suggests that the hydrated ketone is the active form. Taken together, these findings are consistent with previous reports suggesting that γ-secretases are aspartyl proteases with some properties similar to those of cathepsin D.

Because of the elegant explanation offered by the α-helical model for how mutations of position 717 might cause FAD and because the γ-secretase cleavage sites lie well within the postulated membrane boundaries, we favor the hypothesis that the final step in Aβ biosynthesis is an unprecedented intramembranous proteolytic event. The site 2 protease (S2P) involved in the release of the sterol regulatory element binding protein (SREBP) from the endoplasmic reticulum is apparently also cleaved within the transmembrane region of its substrate (*23*), although the exact site of proteolysis has recently been shown to occur close to the junction between the cytoplasmic and transmembrane domains (*44*). Likewise, while the amino acid sequence of cloned S2P suggests a metalloprotease that winds its way through the membrane multiple times, the signature metalloprotease sequence is positioned at the postulated membrane boundary (*45*).[2] Although the idea of an intramembranous hydrolytic event might seem untenable, other integral membrane proteins form channels for the admission of water [e.g., aquaporin (*46*, *47*)], and integral membrane transport proteins function in ways related to the chemical processes carried out by enzymes.

[2] It should be made clear that S2P is not a γ-secretase. Although the parallels between the proteolytic processing of APP and SREBP are striking and it has been suggested that γ-secretase and S2P could be identical, recent studies with S2P-deficient and S2P-overproducing APP-transfected cells have ruled this out (*1*, *2*).

In summary, the peptidomimetic γ-secretase inhibitors reported here are useful molecular probes for this protease, providing evidence for loose sequence specificity and an aspartyl protease mechanism. Furthermore, molecular modeling of the γ-secretase cleavage site as an α-helix, based on the idea that the proteolysis is intramembranous, explains how mutations at APP position 717 could raise the level of $A\beta_{42}$ production and cause FAD. The characterization of γ-secretase as an intramembrane-cleaving aspartyl protease should facilitate the eventual identification of this important and unusual protease.

NOTE ADDED IN PROOF

We have recently found that mutation of either of two conserved transmembrane aspartates in presenilin-1 blocks γ-secretase activity and prevents the normal endoproteolysis of presenilin-1 (*48*). These findings support the hypothesis that the presenilins, polytopic proteins that are mutated in most FAD cases, are themselves γ-secretases, novel intramembrane-cleaving aspartyl proteases activated through autoproteolysis.

ACKNOWLEDGMENT

We thank Dr. Joseph De Los Angeles for helpful advice and assistance with the molecular modeling studies and Dr. Peter Seubert for the monoclonal antibodies used for the ELISA.

REFERENCES

1. Tomita, T., Chang, T. Y., Kodama, T., and Iwatsubo, T. (1998) *Neuroreport 9*, 911−3.
2. Ross, S. L., Martin, F., Simone, L., Jacobsen, F., Deshpande, R., Vassar, R., Bennett, B., Luo, Y., Wooden, S., Hu, S., Citron, M., and Burgess, T. (1998) *J. Biol. Chem. 273*, 15309−12.
3. Selkoe, D. J. (1997) *Science 275*, 630−1.
4. Hardy, J. (1997) *Proc. Natl. Acad. Sci. U.S.A. 94*, 2095−7.
5. Selkoe, D. J. (1994) *Annu. Rev. Cell Biol. 10*, 373−403.
6. Roher, A. E., Lowenson, J. D., Clarke, S., Woods, A. S., Cotter, R. J., Gowing, E., and Ball, M. J. (1993) *Proc. Natl. Acad. Sci. U.S.A. 90*, 10836−40.
7. Iwatsubo, T., Odaka, A., Suzuki, N., Mizusawa, H., Nukina, N., and Ihara, Y. (1994) *Neuron 13*, 45−53.
8. Jarrett, J. T., Berger, E. P., and Lansbury, P. T., Jr. (1993) *Biochemistry 32*, 4693−7.
9. Wolfe, M. S., Citron, M., Diehl, T. S., Xia, W., Donkor, I. O., and Selkoe, D. J. (1998) *J. Med. Chem. 41*, 6−9.
10. Selkoe, D. J., Wolfe, M. S., Ostaszewski, O., and Xia, W. (1998) *Soc. Neurosci.*, Part I, Abstract 8.3.
11. Fehrentz, J.-A., and Castro, B. (1983) *Synthesis*, 676−8.
12. Xia, W., Zhang, J., Kholodenko, D., Citron, M., Podlisny, M. B., Teplow, D. B., Haass, C., Seubert, P., Koo, E. H., and Selkoe, D. J. (1997) *J. Biol. Chem. 272*, 7977−82.
13. Citron, M., Diehl, T. S., Gordon, G., Biere, A. L., Seubert, P., and Selkoe, D. J. (1996) *Proc. Natl. Acad. Sci. U.S.A. 93*, 13170−5.
14. Johnson-Wood, K., Lee, M., Motter, R., Hu, K., Gordon, G., Barbour, R., Khan, K., Gordon, M., Tan, H., Games, D., Lieberburg, I., Schenk, D., Seubert, P., and McConlogue, L. (1997) *Proc. Natl. Acad. Sci. U.S.A. 94*, 1550−5.
15. Seubert, P., Vigo-Pelfrey, C., Esch, F., Lee, M., Dovey, H., Davis, D., Sinha, S., Schlossmacher, M., Whaley, J., Swindlehurst, C., et al. (1992) *Nature 359*, 325−7.
16. Buroker-Kilgore, M., and Wang, K. K. (1993) *Anal. Biochem. 208*, 387−92.
17. Klafki, H., Abramowski, D., Swoboda, R., Paganetti, P. A., and Staufenbiel, M. (1996) *J. Biol. Chem. 271*, 28655−9.
18. Weidemann, A., Konig, G., Bunke, D., Fischer, P., Salbaum, J. M., Masters, C. L., and Beyreuther, K. (1989) *Cell 57*, 115−26.
19. Wild-Bode, C., Yamazaki, T., Capell, A., Leimer, U., Steiner, H., Ihara, Y., and Haass, C. (1997) *J. Biol. Chem. 272*, 16085−8.
20. Cook, D. G., Forman, M. S., Sung, J. C., Leight, S., Kolson, D. L., Iwatsubo, T., Lee, V. M., and Doms, R. W. (1997) *Nat. Med. 3*, 1021−3.
21. Hartmann, T., Bieger, S. C., Bruhl, B., Tienari, P. J., Ida, N., Allsop, D., Roberts, G. W., Masters, C. L., Dotti, C. G., Unsicker, K., and Beyreuther, K. (1997) *Nat. Med. 3*, 1016−20.
22. Hardy, J. (1997) *Trends Neurosci. 20*, 154−9.
23. Sakai, J., Duncan, E. A., Rawson, R. B., Hua, X., Brown, M. S., and Goldstein, J. L. (1996) *Cell 85*, 1037−46.
24. Leonhard, K., Herrmann, J. M., Stuart, R. A., Mannhaupt, G., Neupert, W., and Langer, T. (1996) *EMBO J. 15*, 4218−29.
25. Schroeter, E. H., Kisslinger, J. A., and Kopan, R. (1998) *Nature 393*, 382−6.
26. Higaki, J., Quon, D., Zhong, Z., and Cordell, B. (1995) *Neuron 14*, 651−9.
27. Wang, K. K. (1990) *Trends Pharmacol. Sci. 11*, 139−42.
28. Mellgren, R. L. (1997) *Biochem. Biophys. Res. Commun. 236*, 555−8.
29. Evin, G., Cappai, R., Li, Q. X., Culvenor, J. G., Small, D. H., Beyreuther, K., and Masters, C. L. (1995) *Biochemistry 34*, 14185−92.
30. Ladror, U. S., Snyder, S. W., Wang, G. T., Holzman, T. F., and Krafft, G. A. (1994) *J. Biol. Chem. 269*, 18422−8.
31. Doherty, A. M., Sircar, I., Kornberg, B. E., Quin, J. d., Winters, R. T., Kaltenbronn, J. S., Taylor, M. D., Batley, B. L., Rapundalo, S. R., Ryan, M. J., et al. (1992) *J. Med. Chem. 35*, 2−14.
32. Tischer, E., and Cordell, B. (1996) *J. Biol. Chem. 271*, 21914−9.
33. Maruyama, K., Tomita, T., Shinozaki, K., Kume, H., Asada, H., Saido, T. C., Ishiura, S., Iwatsubo, T., and Obata, K. (1996) *Biochem. Biophys. Res. Commun. 227*, 730−5.
34. Lichtenthaler, S. F., Ida, N., Multhaup, G., Masters, C. L., and Beyreuther, K. (1997) *Biochemistry 36*, 15396−403.
35. Yamazaki, T., Haass, C., Saido, T. C., Omura, S., and Ihara, Y. (1997) *Biochemistry 36*, 8377−83.
36. Haass, C., Koo, E. H., Mellon, A., Hung, A. Y., and Selkoe, D. J. (1992) *Nature 357*, 500−3.
37. Saftig, P., Peters, C., von Figura, K., Craessaerts, K., Van Leuven, F., and De Strooper, B. (1996) *J. Biol. Chem. 271*, 27241−4.
38. Silva, A. M., Cachau, R. E., Sham, H. L., and Erickson, J. W. (1996) *J. Mol. Biol. 255*, 321−46.
39. Parris, K. D., Hoover, D. J., Damon, D. B., and Davies, D. R. (1992) *Biochemistry 31*, 8125−41.
40. James, M. N., Sielecki, A. R., Hayakawa, K., and Gelb, M. H. (1992) *Biochemistry 31*, 3872−86.
41. Veerapandian, B., Cooper, J. B., Sali, A., Blundell, T. L., Rosati, R. L., Dominy, B. W., Damon, D. B., and Hoover, D. J. (1992) *Protein Sci. 1*, 322−8.
42. Takahashi, L. H., Radhakrishan, R., Rosenfield, R. E., Jr., Meyer, E. F., Jr., and Trainor, D. A. (1989) *J. Am. Chem. Soc. 111*, 3368−74.
43. Angliker, H., Anagli, J., and Shaw, E. (1992) *J. Med. Chem. 35*, 216−20.
44. Duncan, E. A., Davé, U. P., Sakai, J., Goldstein, J. L., and Brown, M. S. (1998) *J. Biol. Chem. 273*, 17801−9.
45. Rawson, R. B., Zelenski, N. G., Nijhawan, D., Ye, J., Sakai, J., Hasan, M. T., Chang, T. Y., Brown, M. S., and Goldstein, J. L. (1997) *Mol. Cell 1*, 47−57.
46. Walz, T., Hirai, T., Murata, K., Heymann, J. B., Mitsuoka, K., Fujiyoshi, Y., Smith, B. L., Agre, P., and Engel, A. (1997) *Nature 387*, 624−7.
47. Cheng, A., van Hoek, A. N., Yeager, M., Verkman, A. S., and Mitra, A. K. (1997) *Nature 387*, 627−30.
48. Wolfe, M. S., et al. (1999) *Nature* (in press).

BI982562P